VAPOR-LIQUID PHASE SEPARATOR PERMEABILITY RESULTS

BY

S.W.K. YUAN and T.H.K. FREDERKING

PRINCIPAL INVESTIGATOR: T.H.K. FREDERKING

School of Engineering and Applied Science

University of California, Los Angeles

ANNUAL REPORT

FALL 80 - 9/81

GRANT NCC 2-64

SUPPL. No. 1

PREPARED FOR

NATIONAL AERONAUTICS AND SPACE ADMINISTRATION

AMES RESERACH CENTER

OCTOBER 1981

UCLA-ENG-8134

VAPOR-LIQUID PHASE SEPARATOR: PERMEABILITY RESULTS

By

S.W. K. Yuan and T.H.K. Frederking

PRINCIPAL INVESTIGATOR : T.H.K. FREDERKING

School of Engineering and Applied Science
University of California, Los Angeles

ANNUAL REPORT

Fall 80 to 9-81

GRANT NCC 2-64

SUPPL. No. 1

PREPARED FOR

NATIONAL AERONAUTICS AND SPACE ADMINISTRATION
AMES RESEARCH CENTER

OCTOBER 1981

TABLE OF CONTENTS

I. SUMMARY
of
ACTIVITIES
Suppl. No. 1 (NCC 2 - 64)
FUNDING PERIOD
FALL 80 to 9-30-81

Preceding work up to Fall 1980 has been concerned with development and component testing related to vapor-liquid phase separation by means of thermo-osmosis (= utilization of the thermomechanical effect in He II). For a quantification of important design parameters it is necessary to know the throughput of fluid through porous plugs as a function of controlling variables. Therefore, the past year's activities have been directed at the determination of permeabilities of the sintered porous medium used previously , in particular the temperature dependence of the plug throughput. First, the classical mass permeability above the lambda point has been measured for Newtonian fluid flow. Second, the normal fluid permeability has been evaluated below the lambda point for the non-classical quantum liquid He II. Results are presented in the context of progress in related other areas of porous media transport at small flow rates in the Darcy regime. A comparison of various results points out problems to be solved prior to a satisfactory quantification of design parameters for porous plugs of vapor - liquid phase separation systems.

II. INTRODUCTION

In the previous funding period from March 1, 1980 to September 30, 1980, preliminary design and component development has been carried out. This work has been directed toward a system for vapor-liquid phase separation. The data obtained during this period point out that terrestrial testing is possible under suitable conditions. Goals of operation though pertain to He II storage in space at very low gravitational forces or externally applied inertial forces resulting from controlled maneuvers or system perturbations. The previous test results point out that it is possible to use the particular setup and its components respectively in applications which involve He II in the total or in part of a cryogen system for He^4. The present work is a follow-up effort which has been conducted since November 1980 (at reduced funding rates). It turned out that quantification of several important design parameters is not well established. Therefore, the most important transport parameters ought to be studied in relation to possible factors of influence. The present report describes basic conditions governing the use of sintered porous plugs, as far as their behavior has been accessible from our studies. A quantity of prime interest is the permeability formulated on the basis of Darcy's law

for classical Newtonian fluids. The Darcy permeability has been extended to include static thermo-osmotic conditions at low temperatures in the range of superfluid liquid He II. In addition, the present report refers to related information obtained in part with non-metallic porous media. There are two types of Darcy permeability data, described in Section III subsequent to an outline of experimental conditions. The first one is the classical permeability referring to mass throughput of Newtonian fluids above the lambda temperature. The second one is a modified permeability of "normal fluid" below the lambda temperature. Conclusions from this work are presented in Section IV.

III. DARCY PERMEABILITY EXPERIMENTS

The temperature range covered in the present experiments extends from about 300 K to approximately 4.2 K in the area of classical Newtonian fluid flow. The mass throughput $\dot{m}$ is accompanied by a pressure drop ΔP, and a pressure gradient (ΔP) respectively. As long as laminar flow is maintained, there exists a linear relation between $\dot{m}$ and ΔP for a specified temperature T and P with $\Delta P << P$. Darcy's law is most frequently written in terms of the superficial flow speed $\overline{v_o}$ which is the ratio of the volumetric flow rate, $\dot{V} = \dot{m}/\rho$, to the total plug area A_{TOT}; (ρ density of the fluid). Thus, Darcy's law may be written in terms of the permeability K_p as

$$\frac{\dot{m}}{\rho \cdot A_{tot}} = \overline{v_o} = K_p(T,P) \cdot |\nabla P| / \eta \qquad (1)$$

(η shear viscosity).

Experimental systems. Mass flow rates have been measured downstream with either a wet test meter or floating sphere meters. The pressure drop has been measured with either a differential Bourdon gage or a pressure transducer (Validyne model CD 23, diaphragm No. 20). The plugs used in the present work were all from Mott Metallurgical

Corporation with a nominal pore size of 2 μm and a plug diameter (overall) of 1 in. = 2.54 cm, and a plug thickness of 1/8 in. = 0.317 cm.

The system for classical fluid tests (Fig. 1) allows the admission of He^4 gas from a compressed gas cylinder. The He^4 passes first through heat exchangers inside the dewar vessel containing the plug. A vacuum pump is connected initially for the evacuation of the plug system. Subsequently, during measurements with He^4 gas, the downstream of the plug side is connected to the flow meter system. Either liquid nitrogen or liquid He I is used at the bottom of the dewar vessel during low temperature runs. Data are taken during slow cool-down rates which permit quasi-steady operation. After the system has reached the vicinity of the boiling point of the cryo-liquid, data are taken during slow warm-up of the system to the previous temperature. During initial runs at room temperature the entire system is nearly isothermal. In the high temperature range chromel-constantan thermocouple thermometry is employed (as indicated schematically in Figure 1). At low temperatures close to the liquid He I bath temperature, a carbon thermometer is used (Allen Bradley, 1/8 Watt, 39 Ohm nominal resistance at room temperature).

In Figure 2, the setup for thermo-osmotic phase separation is shown schematically. Mass throughput occurs

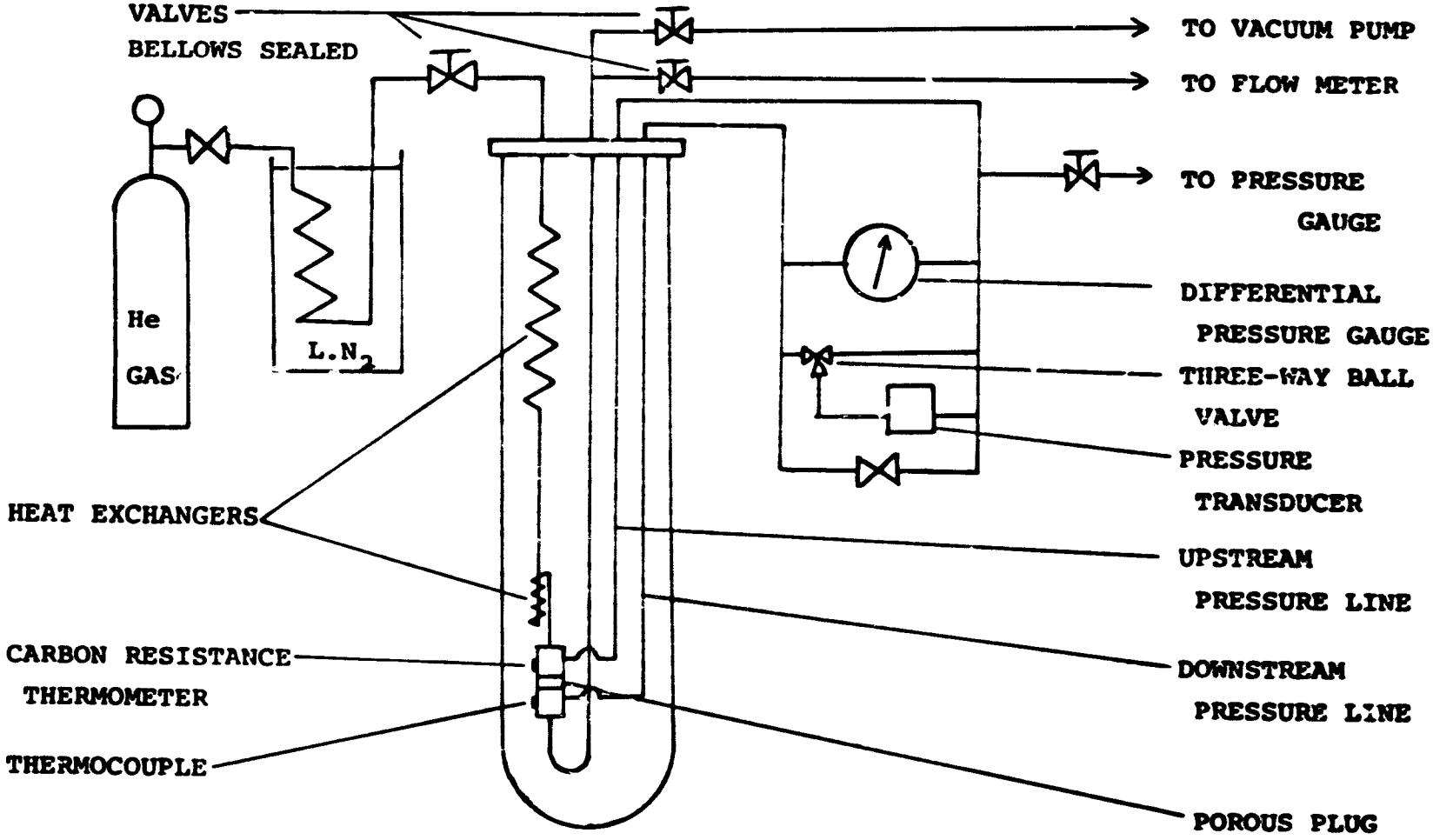

Figure 1. System for permeability measurements of classical fluid flow (schematically).

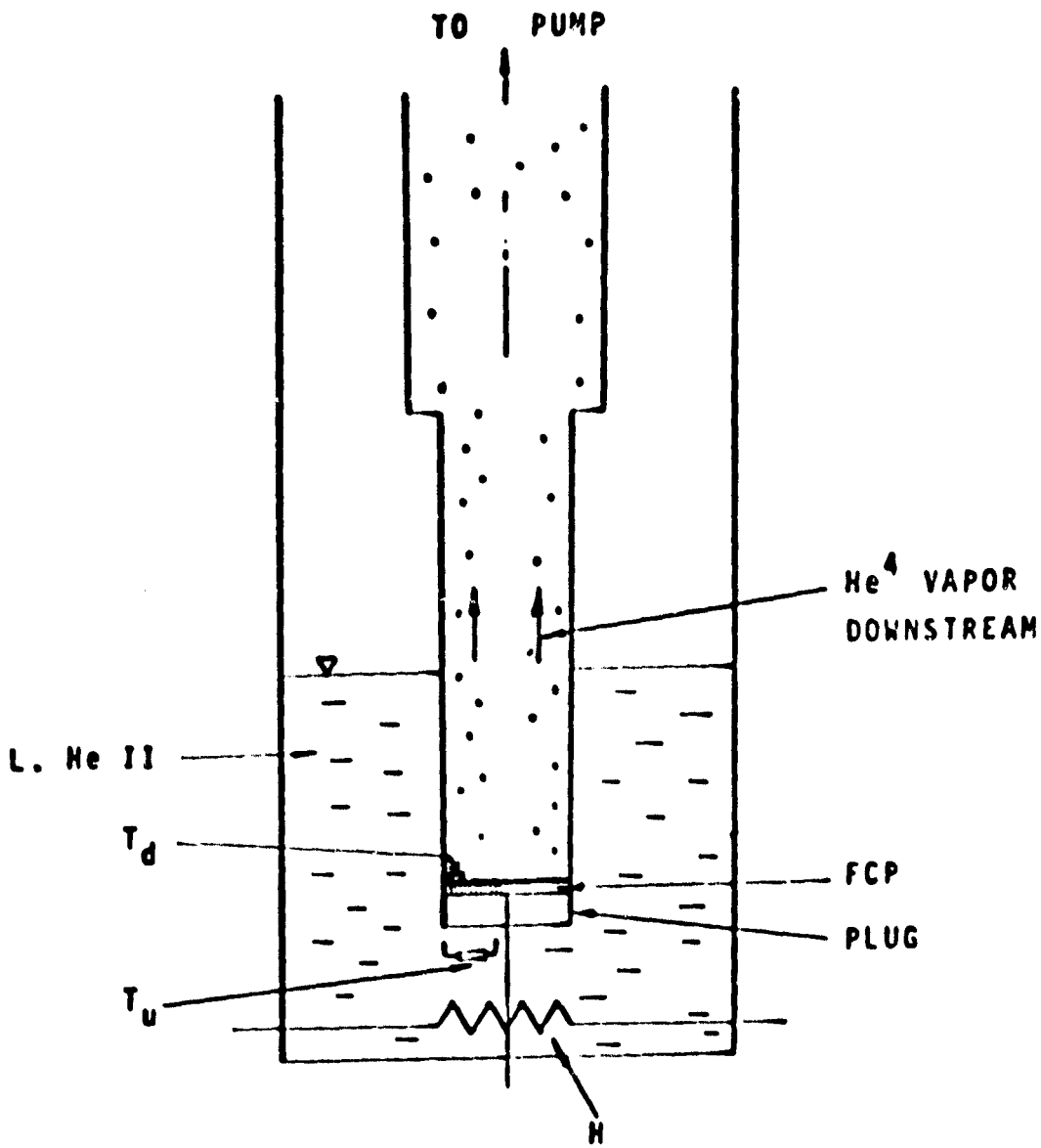

FCP FLOW CONTROL PLATE
T_u UPSTREAM TEMPERATURE
T_d DOWNSTREAM TEMPERATURE

FIG. 2 Schematic of the low temperature system.

from the outside bath to the central inner tube via the plug. In other words, the liquid surrounding the central tube is the upstream location as far as mass throughput through the plug is concerned, and the inner tube is the downstream side. This type of flow also pertains to the heat rejection rate through the plug. Vapor emerges from the upper side of the plug and is pumped away to the top of the duct. In contrast to the classical fluid runs (Fig. 1), there is a flow control plate (FCP in Fig. 2), located downstream of the plug, i.e. on top of the plug. The flow control plate contains 40 holes. Thus, only a small cross section is available nominally. Measurements of the throughput are evaluated on the basis of a modified Darcy law based on the normal fluid speed and the driving thermo-osmotic pressure gradient. These will be described subsequent to the classical permeability measurements conducted with the system of Figure 1.

Classical fluid permeabilities. The classical fluid experiments covered runs with both systems, the setup of Figure 1, and the thermo-osmotic system of Figure 2.

Figure 3 represents data at room temperature at relatively small mass throughputs, and Figure 4 shows data over an extended range in throughput and ΔP. When the mass flow rate is kept constant, a lowering of T results in an increased volumetric flow rate. When $\overline{v_0}$ is very large, the transition from laminar to turbulent flow may take place. When large

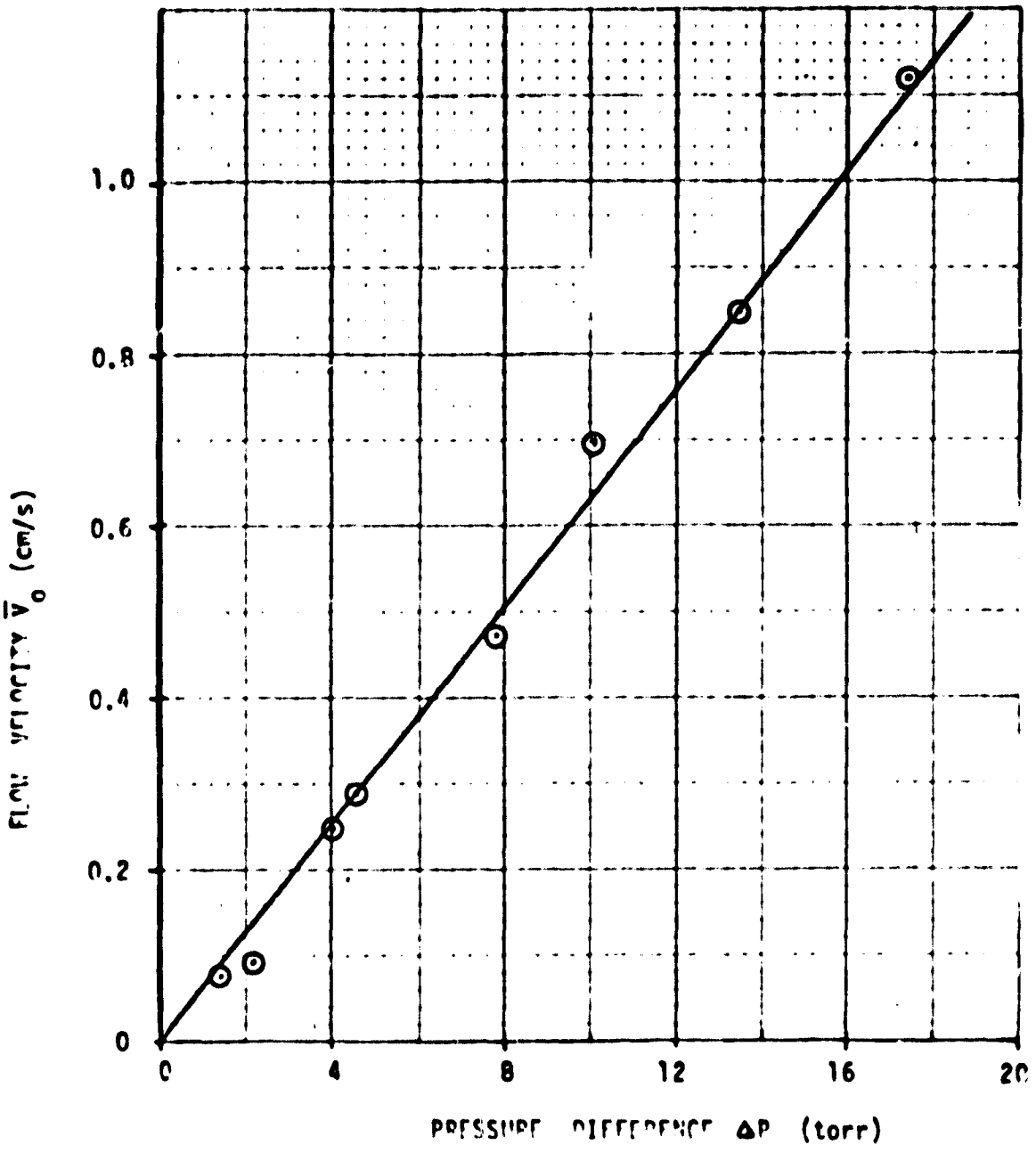

FIG.3 . $\bar{V}_0$ vs ΔP at liquid helium temperature.

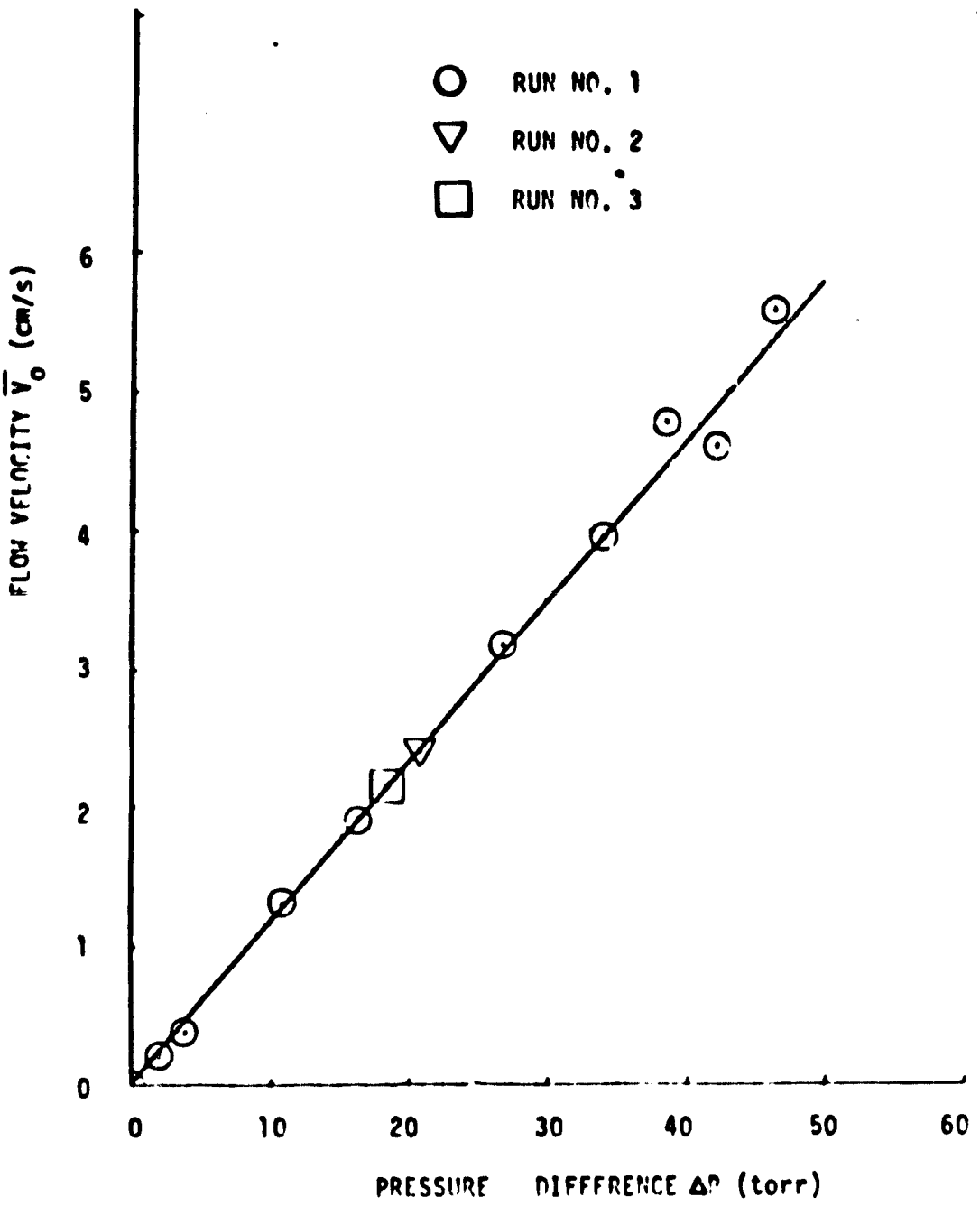

Figure 4. Speed $\overline{v_o}$ versus ΔP at room temperature

amounts of He^4 gas pass through the system, however, there is another possibility. The heat exchanger system may function off the design point. This results in a higher temperature and an apparent permeability which is lower than K_p-values extrapolated from the linear function at low $\dot{m}$.

Figure 5 is an example of liquid nitrogen runs with a non-linear behavior of the superficial speed versus pressure difference. It is noted that the Reynolds number in Figure 5 is lower than the limit of laminar flow. At large mass flow rates, the heat exchanger does not function in the design range and the temperature rises. Insertion of the property values at the liquid nitrogen temperature leads to a $\overline{v_o}$-value which is too low. Thus, the apparent permeability resulting from this procedure will be smaller than the real permeability. Therefore, the fluid temperature has to be known to obtain density and viscosity in Equation (1), and subsequently the permeability. Data obtained in this manner are shown in Figure 6 for an extended temperature range.

The permeability studies described subsequently refer to the apparatus shown in Figure 2. This setup incorporates a flow restriction created by the flow control plate which is essentially a perforated G-10 plate. There are 40 holes with a diameter D_h = 0.159 cm (= 1/16 in.). Prior to the low tem-

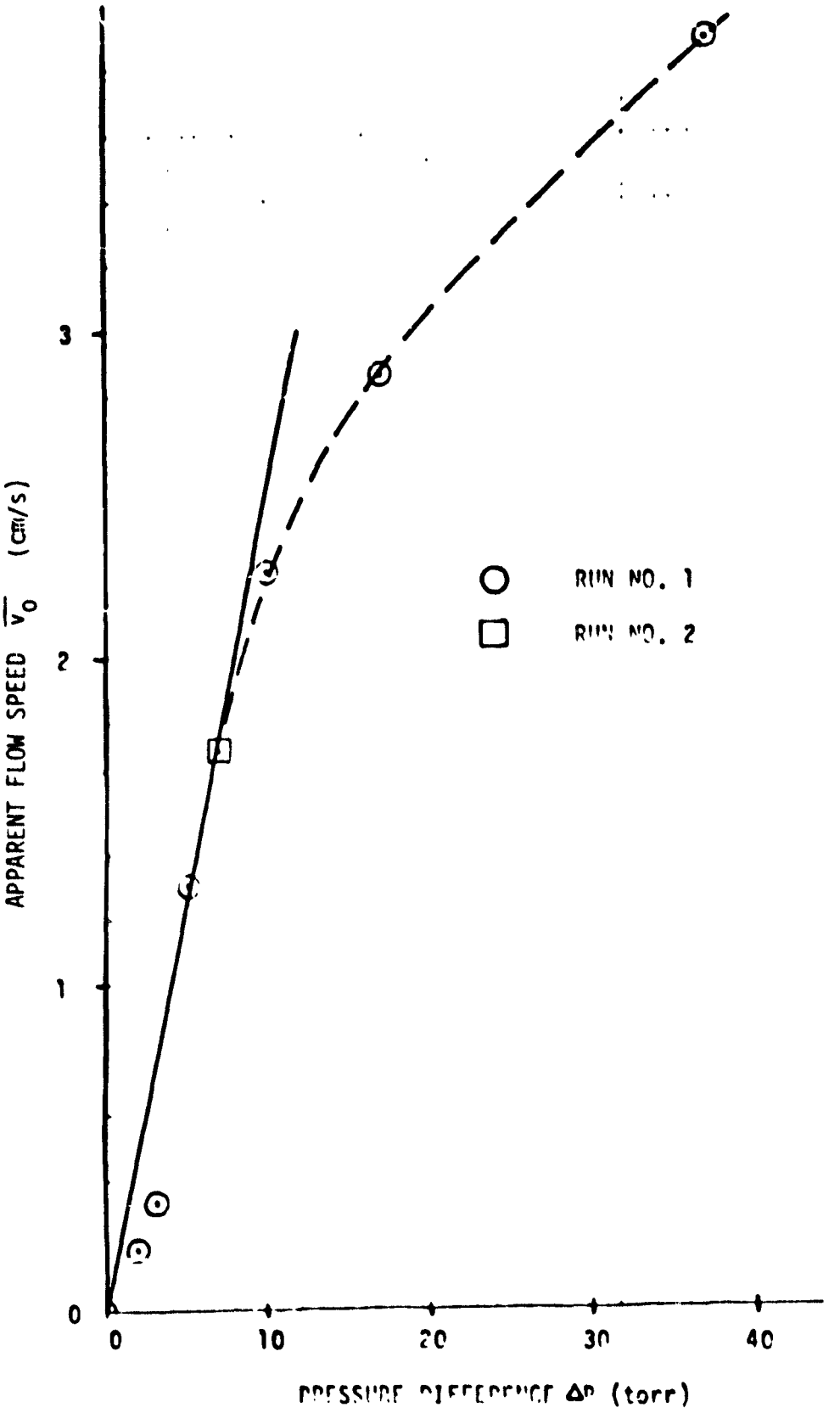

FIG. 5 . $\bar{V}_o$ vs ΔP at liquid nitrogen temperature.

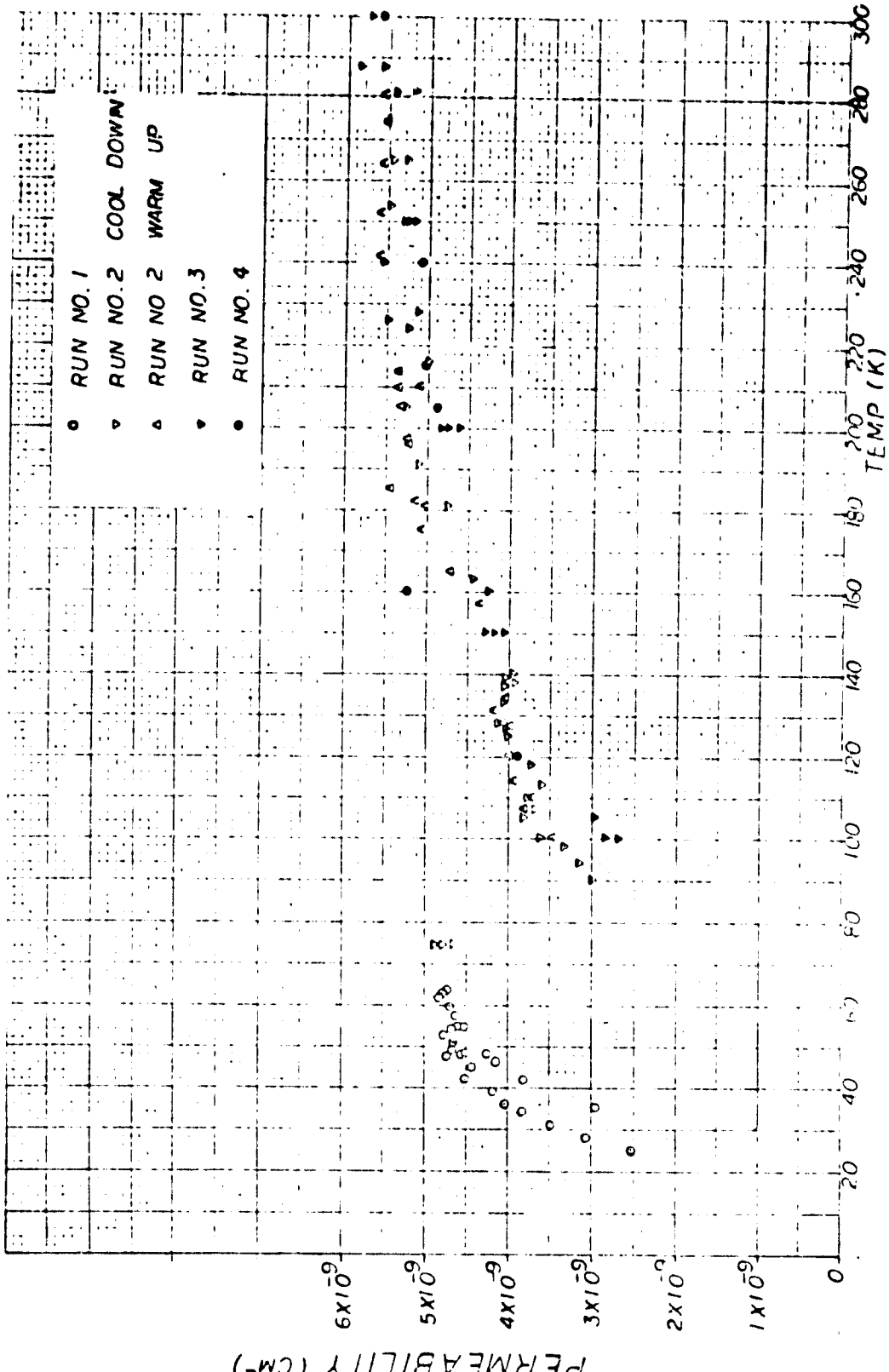

Figure 6. Permeability as a function of temperature

perature runs, this system's permeability has been measured at room temperature with He^4 gas.

Figure 7 is a schematic drawing of the flow pattern expected in the vicinity of a single hole. In general, radial flow components are expected because of the "rough" boundary of the porous plug. In order to minimize these flow components, an intermediate filter material has been inserted. It is noted that the flow control plate is located downstream as far as mass flow is concerned. The liquid upstream contains the entropy carriers (normal fluid) involved in the transport process, which occupy a larger cross section than the hole cross section. The total cross section is $A_{tot} = A_1 \cdot N$; (N = number of holes = 40; $A_1 = (\pi/4)D_h^2$ = cross section of a single hole.) This enlargement of the flow cross section has been expressed in terms of an equivalent diameter D_{eq} sketched in Figure 7.

From the previous measurements at 300 K and additional data, the plug permeability at room temperature is known to be $K_p(300) = 5 \times 10^{-9}$ cm^2. This value pertains to the 1 in. plug with a total area of 5.06 cm^2. From the data in Table I and $K_p(300)$, the effective area $A_{eff} = 3.2$ cm^2 is calculated for the configuration of Figure 7 with the flow control plate in place.

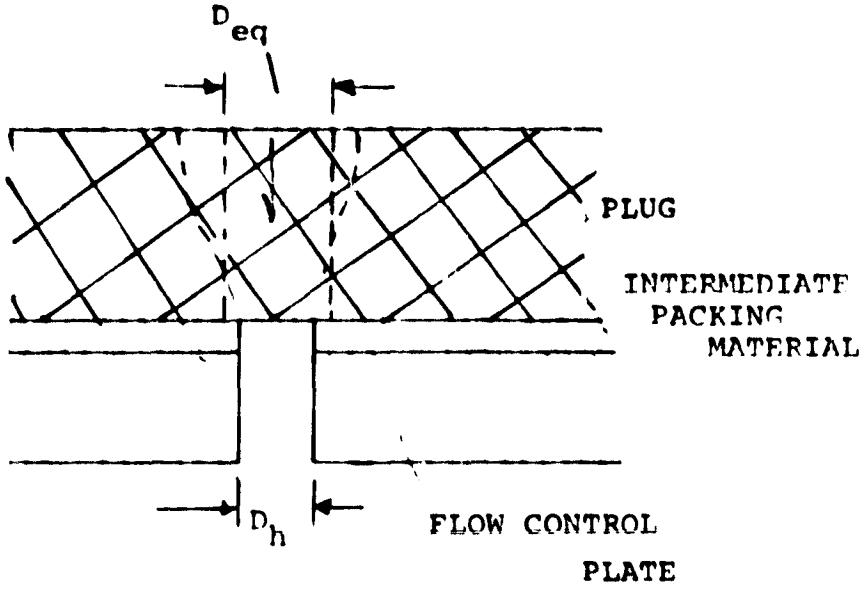

Figure 7. Plug with flow control plate: Single hole geometry (shown schematically, configuration turned 180 degrees).

D_{eq} = equivalent diameter

D_h = hole diameter

TABLE I. Room temperature data for restricted area system (Figure 7)

RUN #	P, torr	$\dot{V}$, cm^3/s
1	16.8	5.48
2	21.5	6.95
3	26.2	8.59
4	29.5_5	10.1

From the total hole cross section $A_{tot} = (40)x(0.0198\ cm^2) = 0.794\ cm^2$, a ratio of the effective area to A_{tot} of 4.03 results. This corresponds to an equivalent diameter (Fig.7) of $D_{eq} = 2.01D_h$. After these room temperature runs, the thermo-osmotic permeabilities at low temperature have been determined.

Thermo-osmotic permeabilities associated with normal fluid transport.

Measurements of the throughput at liquid He II temperatures have been conducted with the apparatus of Figure 2. These data are evaluated on the basis of the modified Darcy law. The mass flow speed $\overline{v_o}$ in Eq. (1) is replaced by the normal fluid flow speed (superficial value $\overline{v_{no}}$). This speed is obtained from the superficial heat flow density,

$$\overline{q_o} = \rho\ S\ T\ \overline{v_{no}}\ . \qquad (2)$$

(S, entropy per unit mass of liquid He^4; ρ density of liquid He^4.) The pressure gradient driving normal fluid toward the "heat sink" is the thermo-osmotic gradient. This driving quantity is related to the temperature gradient ∇T, established across the plug by London's equation,

$$\nabla P_T = \rho S \nabla T . \tag{3}$$

The shear viscosity of classical fluids is to be replaced by the shear viscosity of the normal fluid η_n. Thus, the permeability of normal fluid transport through the porous medium is expressed in terms of the following modified Darcy law as

$$K_{pn} = \overline{v_{no}}\ \eta_n / |\nabla P_T| \tag{4}$$

or

$$K_{pn} = (\overline{q_o}\ \eta_n / [(\rho S)^2\ T\ |\nabla T|\ ] . \tag{5}$$

External imposition of a temperature difference is achieved by vapor pressure (P_v)-control using a difference ΔP_v. As long as the pressure difference is small, i.e., $\Delta T << T$, the Clausius-Clapeyron equation relates ΔT to ΔP_v.

$$\Delta T = \Delta P_v\ T/(\rho_v \lambda);\ \rho_v << \rho_L \tag{6}$$

(ρ_v density of saturated vapor, ρ_L density of saturated liquid, λ latent heat of vaporization).

Data of the thermo-osmotic runs with the apparatus of Figure 2 are shown in Figure 8. This figure presents the normal fluid permeability $(K_p)_n$ as a function of temperature for the conditions of heat supply rates specified. The flow control plate - plug assembly is assumed to be characterized by the same degree of throughput effectiveness which has been encountered at room temperature . In other words, the equi - valent diameter of Figure 7 has been inserted in the nominal cross sectional area used in the calculations. The transport quantity $(K_p)_n$ is seen to be a strong function of temperature. At the low temperature end accessible, permeability values of the order of magnitude of the room temperature permeability are reached. For an assessment within the frame of reference given by other related results, a comparison of literature data with the present findings appears to be appropriate.

Comparison with literature data. Theoretical interpretation of very recent work has been presented by Schotte et al. [1]. This effort aims in most of its aspects at an understanding of the active phase separator of Klipping et al. [2]. This type of phase separator contains a movable pin-like element which permits variation of the fluid cross section of the separator. As far as porous media work is concerned, the JPL-group has reported results in Reference 3 . Additional plug data have been collected by the Huntsville group[4] in conjunction with a liquid He transfer system.

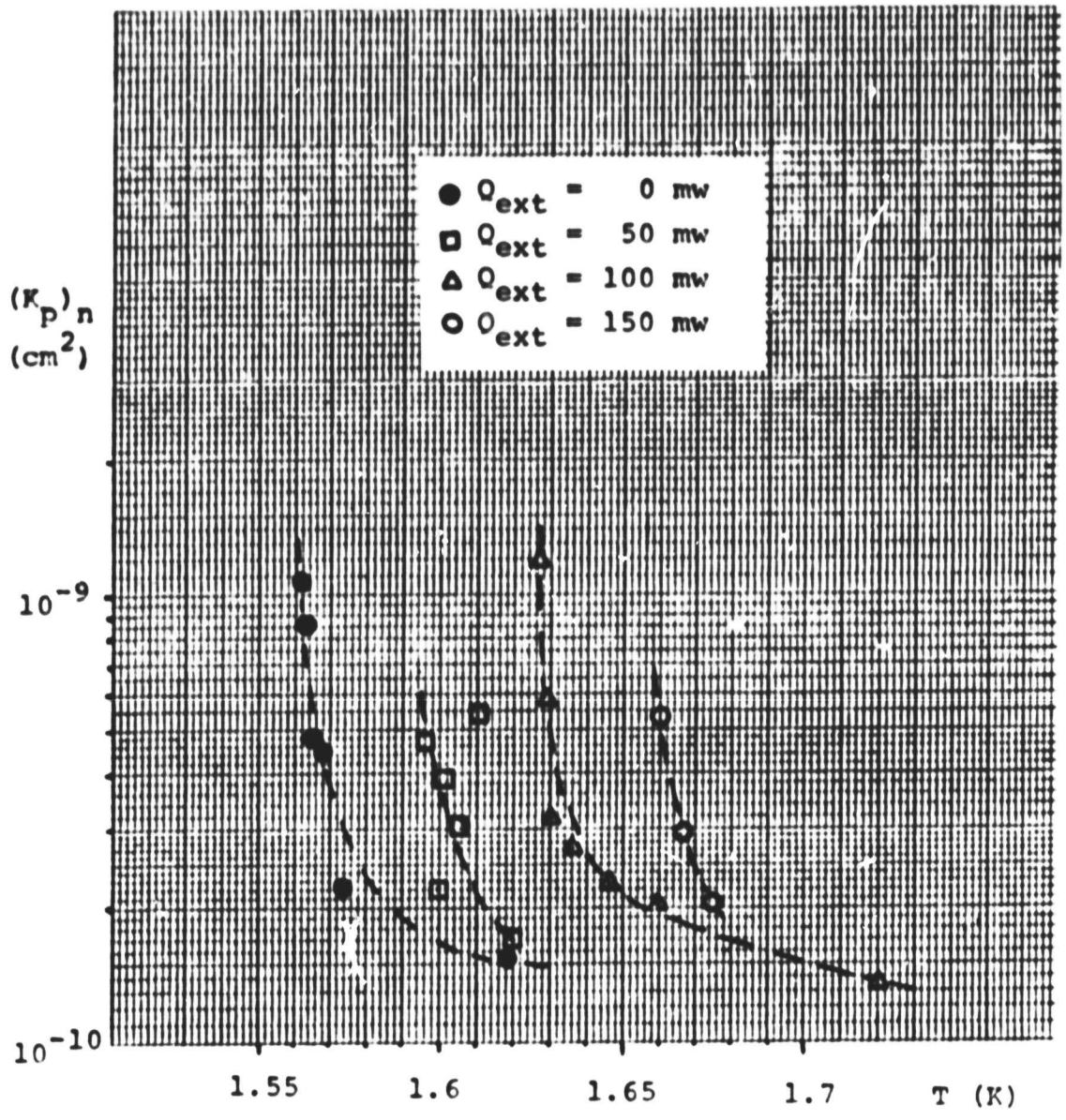

Figure 8 . Normal fluid permeability $(K_p)_n$ as a function of liquid bath temperature.

The overall equipment performance may be compared on the basis of the pressure drop as a function of temperature and externally applied heat, and mass throughput respectively. Figure 9 is an example of data reported by Becker et al.[5], and Figure 10 displays the data of the system shown in Figure 2. It is seen that there exists qualitative similarity. Quantitatively the system of Reference 5 permits small pressure drops at low T. In general the small pressure differences reflect low mass throughputs and small heat rejection rates.

The permeability of sintered plugs may be well defined for large particle diameters when the particles are close to spherical shape. The data of Robinson [6] and Hall[7] for sintered tungsten have been compared[9] with packed bed conditions for near - spherical particles in Figure 11. The equation of Ergun [8], used in this comparison, takes into consideration the porosity (ε) and the particle diameter D_p. Its permeability may be expressed as

$$K_p = 5.5 \cdot 10^{-3} \cdot D_p^2 \, \varepsilon^3 / (1-\varepsilon)^2 \qquad (7)$$

According to Figure 11, the Ergun equation is seen to be quite a reasonable approximation in the particle range above the order of magnitude of 10 μm.

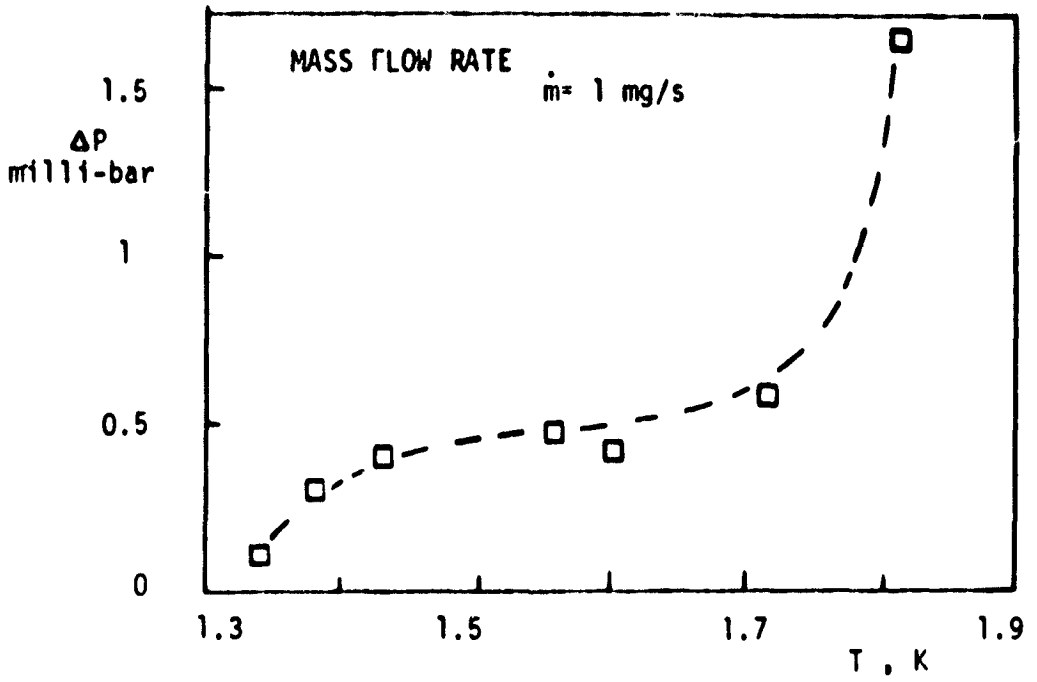

Figure 9. Pressure drop across plug as a function of temperature; Example : Investigations of Becker et al.[5] .

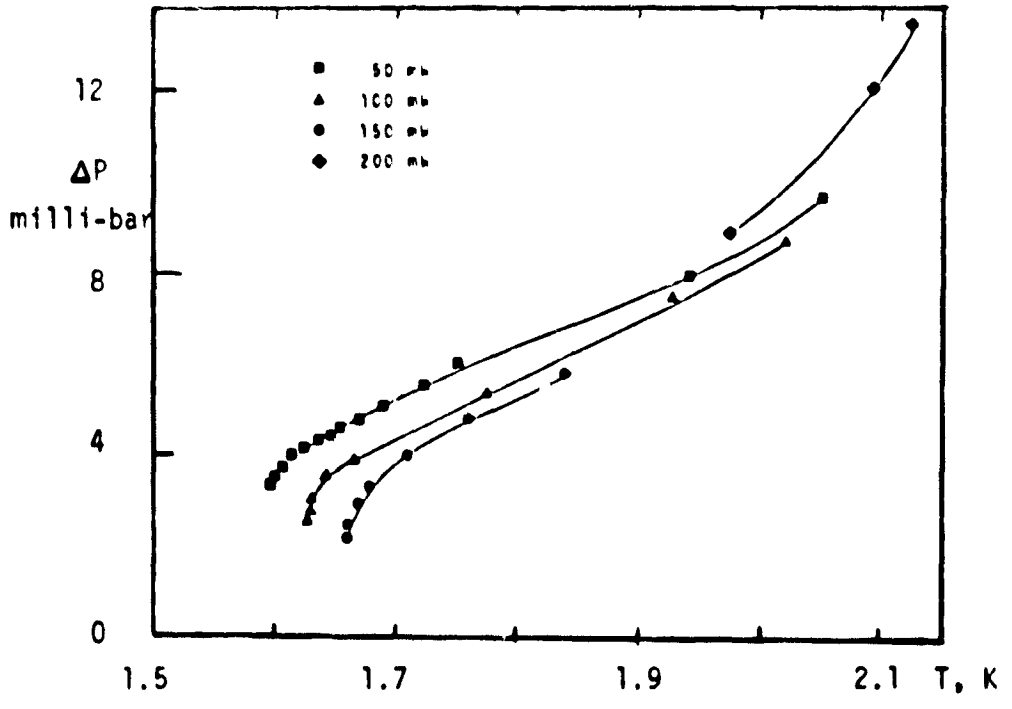

Figure 10. Pressure difference across plug of Figure 2 for various externally applied heating rates.

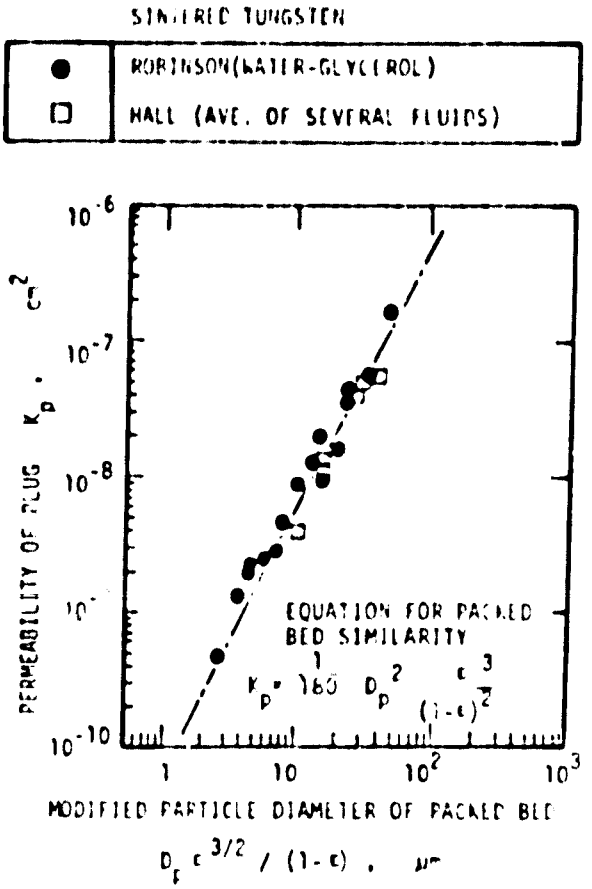

Figure 11. Permeability of sintered tungsten plug materials vs. modified diameter of near-spherical particle beds;

Reference: Ergun equation for packed beds [8], in the limit of small $\Delta P \ll P$.

Data compilation of Reference 9.

A somewhat different picture is presented in Figure 12 for the particle diameter range below the order of 10 μm . According to Ergun's equation, the permeability is proportional to D_p^2 , or the square root of K_p is pro - portional to the particle diameter $D_p = 2 R_p$. Figure 12 indicates that below ,10 μm the size dependence is weaker than the prediction on the basis of Equation (7). One reason for this behavior may be related to the difficulty of getting a uniform set of particles remaining spherical in shape during the sintering process despite the small particle diameter.

Figure 13 shows the square root of the permeability versus the pore size of non-metallic sintered plugs re- ported in recent years in the literature. It appears, to first order, that a functional dependence of $K_p^{1/2} \sim s_o$ may be useful for data description;(s_o = pore size). The points in Figure 12 are based however on only a restricted set of data. There are three different plugs. The 1-micron plug is Al-silicate of Klipping et al.[10] with a permeability of 1.04×10^{-11} cm^2, based on room temperature measurements with dry air. The intermediate size is the 5-micron plug of Reference 4 with 5.05×10^{-10} cm^2 . The 10-micron system is a glass plug[10] with a permeability of 3.4×10^{-9} cm^2. measured at room temperature with dry air. For the 5-micron plug He^4 gas flow at atmospheric pressure has been used.

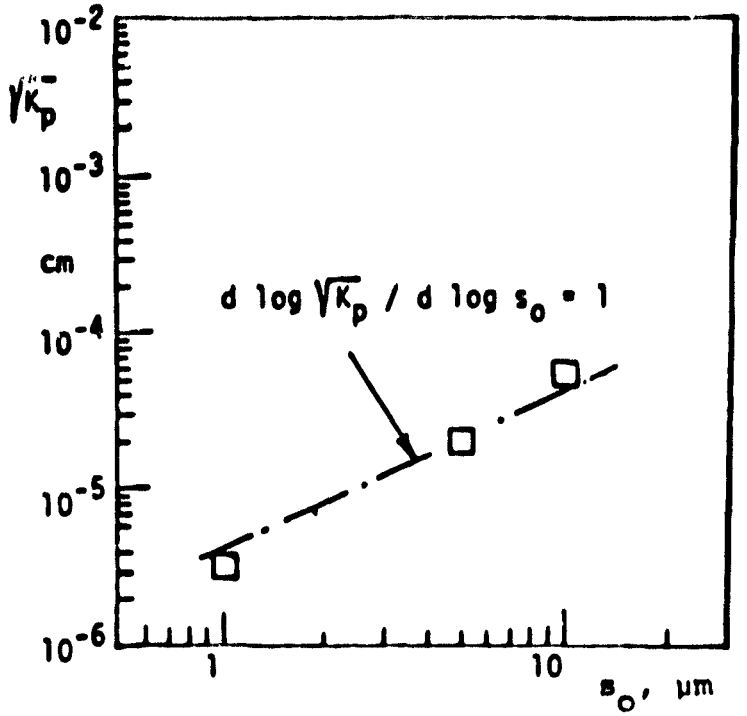

Fig.13. Square root of permeability versus nominal pore size (s_o) for sintered non-metallic plugs.

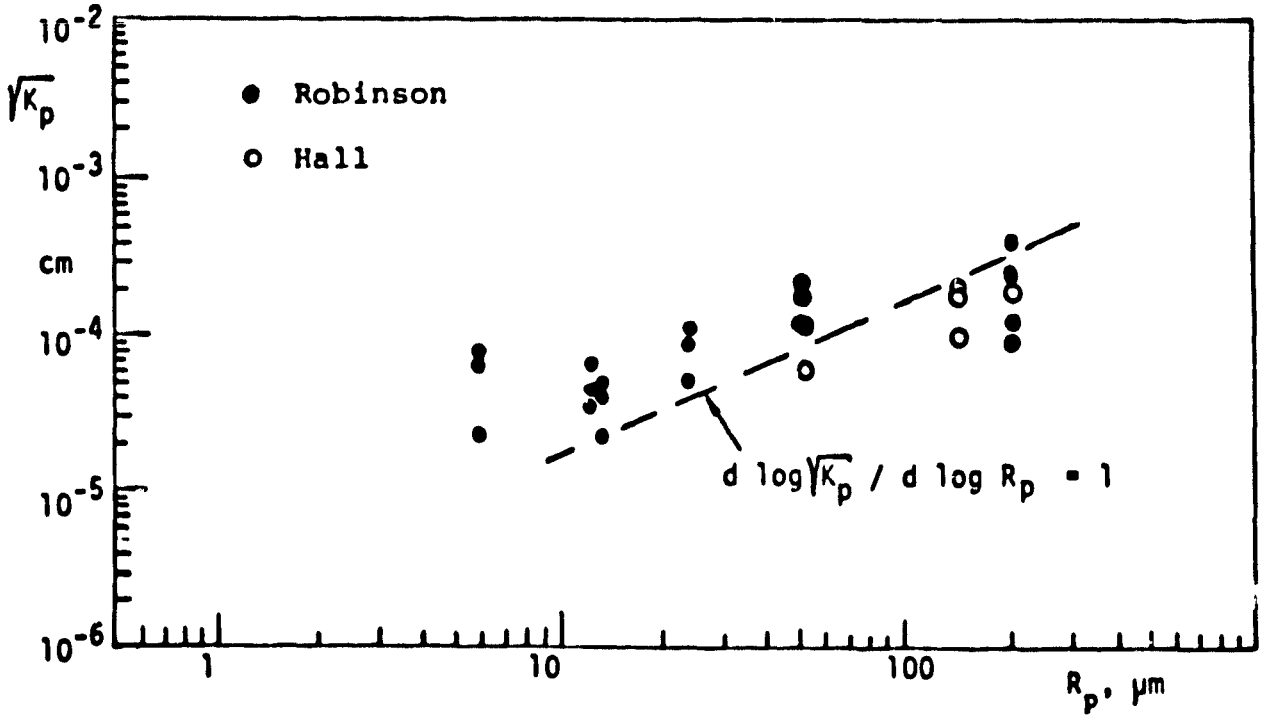

Fig.12. Square root of the permeability versus particle radius R_p for sintered tungsten.

Part of these data quoted are results recalculated on the basis of limited information made available, and in part based on different throughput definitions. Therefore, the uncertainty is larger than apparent from the plot in Figure 13. Another reason for low reliability of this type of information resides in the fact that the pore size is a number quoted with one or at most two digits in the small size range. This quantity is not very well defined. An example of this type of information has been given by Urbach et al.[11] who report that a five-micron size plug may have a pore size significantly larger than the nominal value 5 micron.

Another interesting point in porous media property assessment is the low temperature behavior at zero net mass flow when $\Delta T \ll T$. This case appears to be understood better than the vapor-liquid phase separation mode as there are much larger data sets available in the literature. Recent examples are References 12 and 13. Figure 14 presents two data sets of this work. It is seen that there exists a well-defined normal fluid permeability at zero net mass flow. Thus, this type of data suggests that, at least in principle, it should be possible to evaluate parameters of prime interest in the prediction of low temperature operation of porous media.

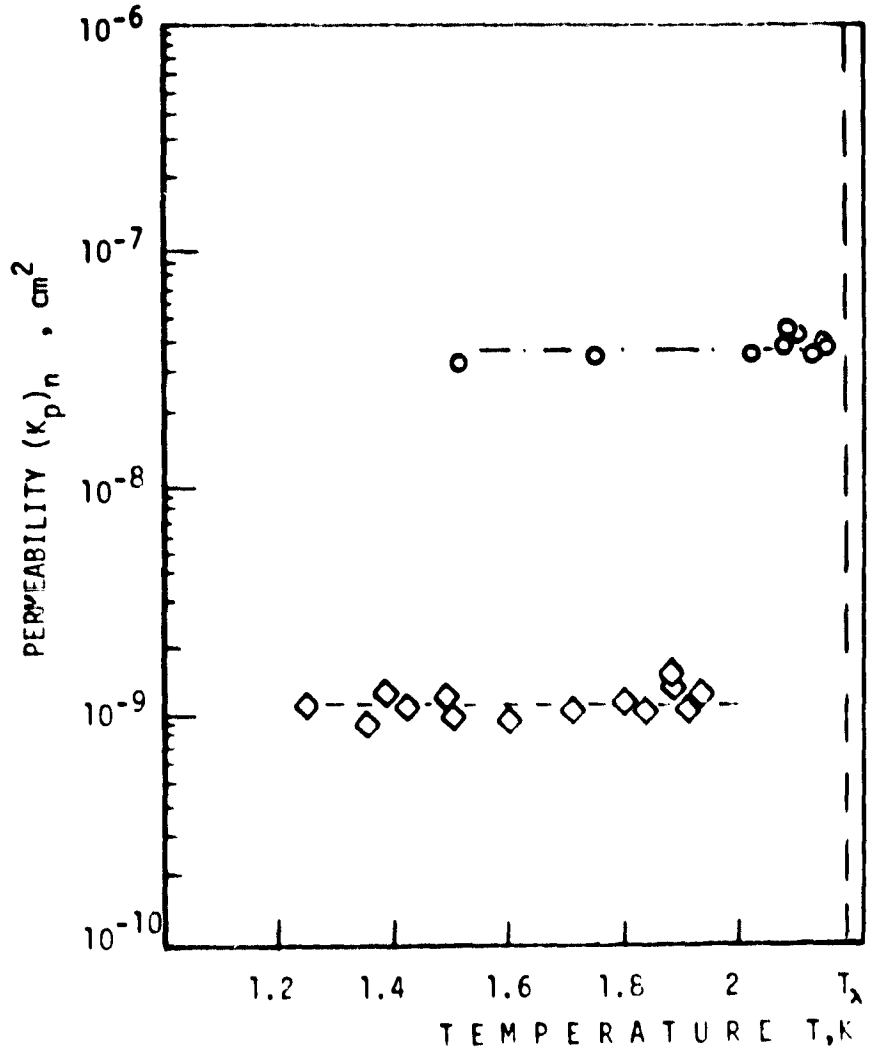

Figure 14. Normal fluid permeability at zero net mass flow;
◇ Data of Schmidt-Wiechert [12];
o Data of packed material of Reference 13.

IV. CONCLUSIONS

From the present evaluation of porous plug throughput it is concluded that the lack of a detailed porous media characterization at present rules out a quantitative description for design purposes. One point to be clarified in greater detail is the temperature dependence in both regimes, first during Newtonian fluid flow, and second, during low temperature transport of normal fluid subjected to vapor-liquid separation constraints. However the few data obtained for mass throughput and thermo-osmotic normal fluid throughput are encouraging in so far as there appear to be well-defined trends for various constraints imposed. Thus, a better material clarification is expected to be possible on the basis of systematically collected experimental data.

Acknowledgment. Various inputs and contributions of Dr. C. Chuang and Messrs. Y.I.Kim, Y. Kamioka, and Jeffrey M. Lee are gratefully acknowledged.

REFERENCES

1. U. Schotte and H.D. Denner, ICEC 8, IPC Sci. Technol. Press, 1980, 27; U. Schotte, Physica 107B, 577, 1981.

2. K. Luders and G. Klipping, ICEC 8, IPC Sci. Technol. Press, 1980, 14.

3. D. Petrac and P.V. Mason, ICEC 8, IPC Sci. Technol. Press, 1980, 97; ICEC 7, IPC Sci. Technol. Press, 1978, 120.

4. G.R. Karr and E.W. Urban, Cryogenics 20, 266, 1980.

5. J.R. Becker, P. Blaser, M. Perdu and R. Prost, ICEC 8, IPC Sci. Technol. Press, 1980, 22.

6. A.T. Robinson, Trans. of the ASM, 57, 650, 1964.

7. R.B. Hall, M.Sc. thesis, Univ. California, Los Angeles 1967.

8. S. Ergun, Chem. Eng. Progr. 48, 89, 1952.

9. C. Chuang, Y.I. Kim and T.H.K. Frederking, in"Cryog. Proc. Equipm. in Energy Systems", ASME Publ. No. H 00164,1980.

10. H.D. Denner, G. Klipping , I.Klipping, J. Menzel and U. Ruppert, Cryogenics 18, 166, 1978 .

11. A.R. Urbach, P.V. Mason and W.F. Brooks, Cryog. Eng. Conf. San Diego 1981, paper BE-2.

12. R.Schmidt and H. Wiechert, Z. Physik B 36, 1, 1979.

13. T.H.K. Frederking, H. van Kempen, M.A. Weenen and P. Wyder, Physica 108 B, 1129, 1981.

APPENDIX A

PROPERTY GRAPHS - HELIUM-4

During the runs above 5 K , He^4 gas has been used for the permeability measurements. In this work the shear viscosity η and the density ρ of He^4 gas are needed at atmospheric pressure. This gas state is close to ideal gas conditions. In addition, it is useful to calculate heat input and output of various components. Therefore, values of the Prandtl number (Pr) and the thermal conductivity are useful. The graphs have been based upon the NBS Techn. Note 631 by R.D. McCarty, Nov. 1972.

At He II temperatures, i.e. below the lambda point, thermo-osmotic parameters have been evaluated using the set of property data reported by J. Maynard for thermodynamic equilibrium (Phys. Rev. B 14, 3868, 1976). In addition the shear viscosity of the normal fluid is required for the permeability of the normal fluid. A large uncertainty in η_n is seen in the Figure compiled by S.C. Soloski (Ph.D. thesis, UCLA 1977). In the calculations a smooth function,proposed by Soloski, has been used.

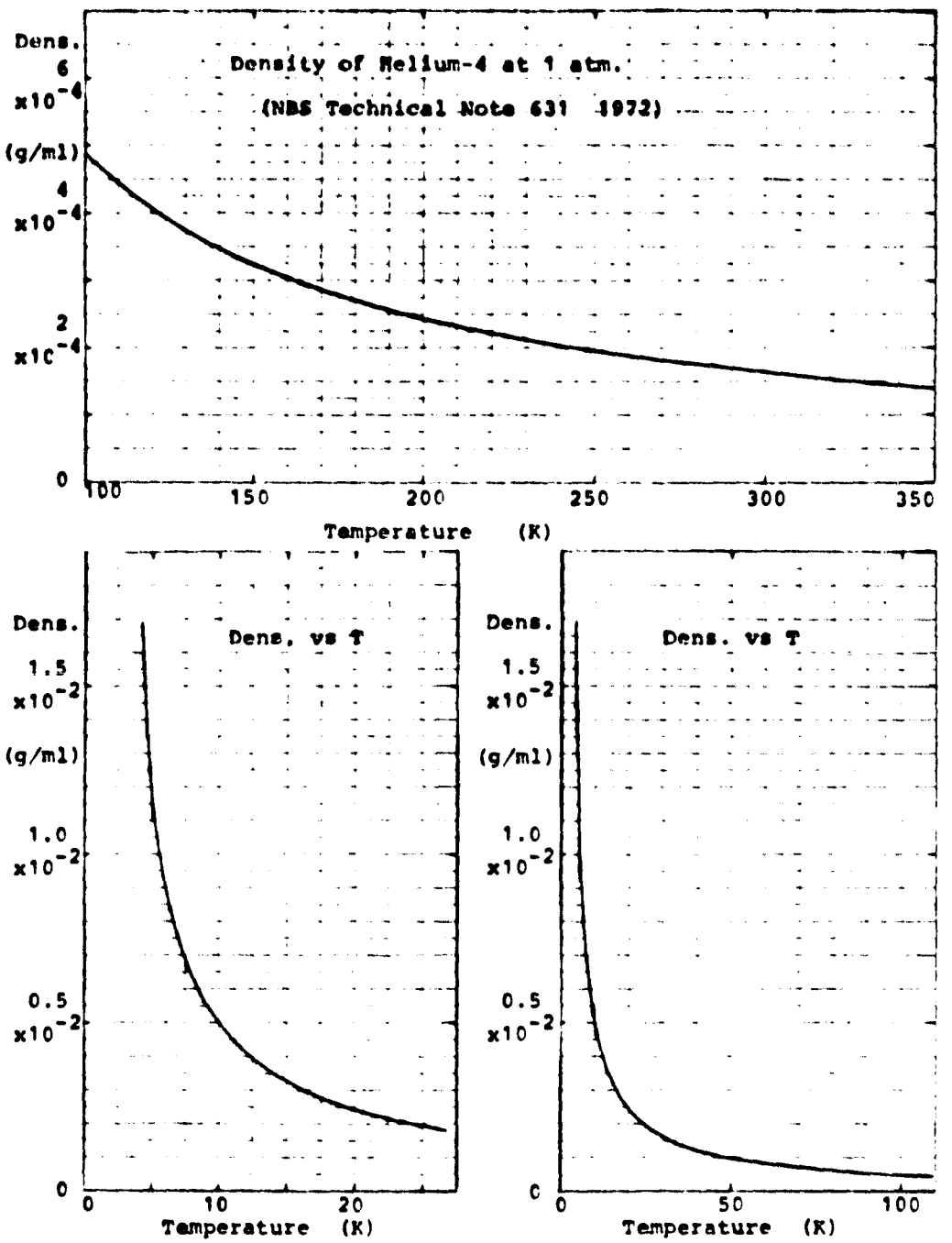

Figure A-1. Density of Helium-4 at 1 atm.

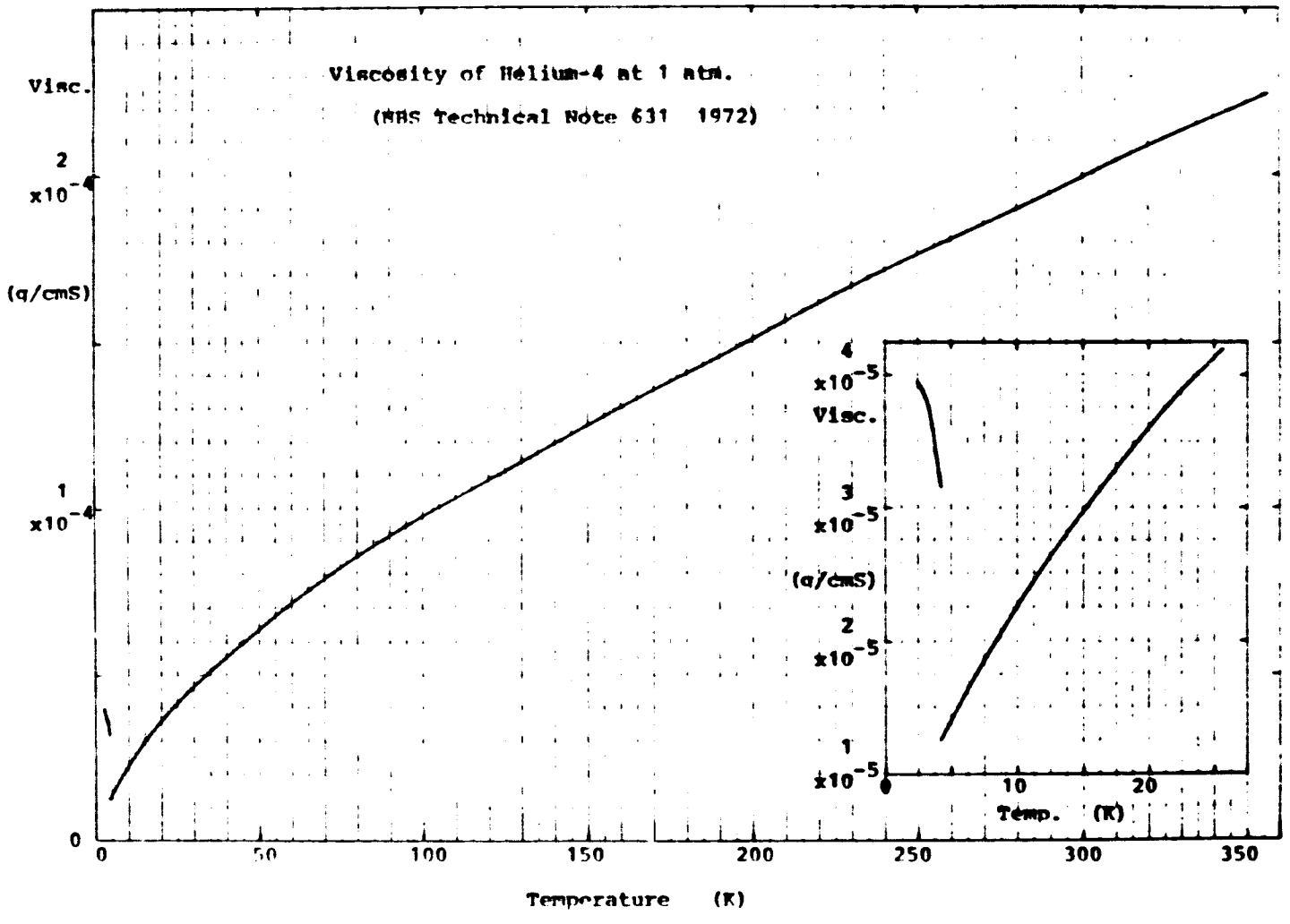

Figure A-2 . Shear viscosity of Helium-4 gas and fluid resoectively.

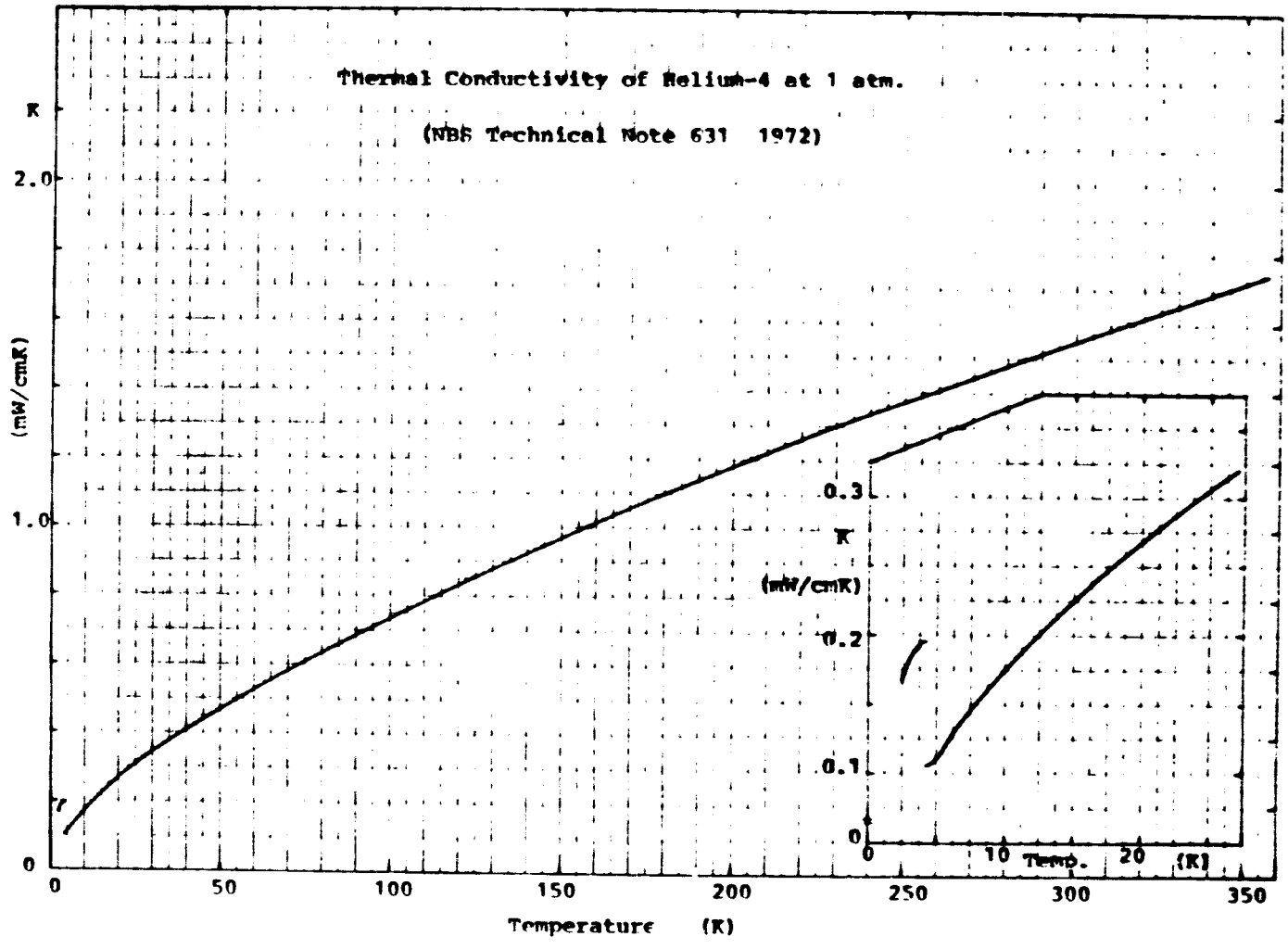

Figure A-3. Thermal conductivity of Helium-4 at 1 atm.

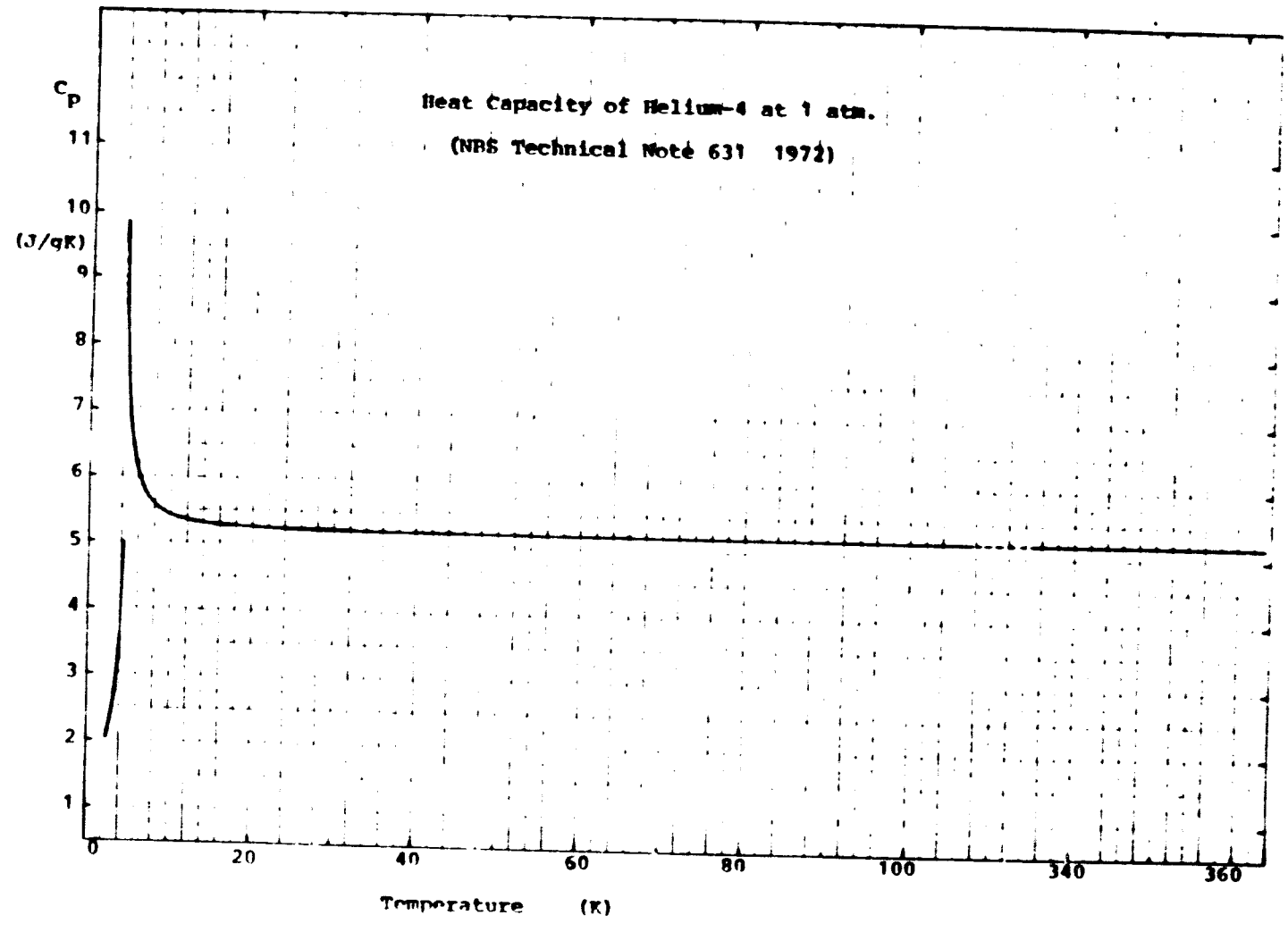

Figure A-4. Specific heat at constant pressure of Helium-4 at 1 atm.

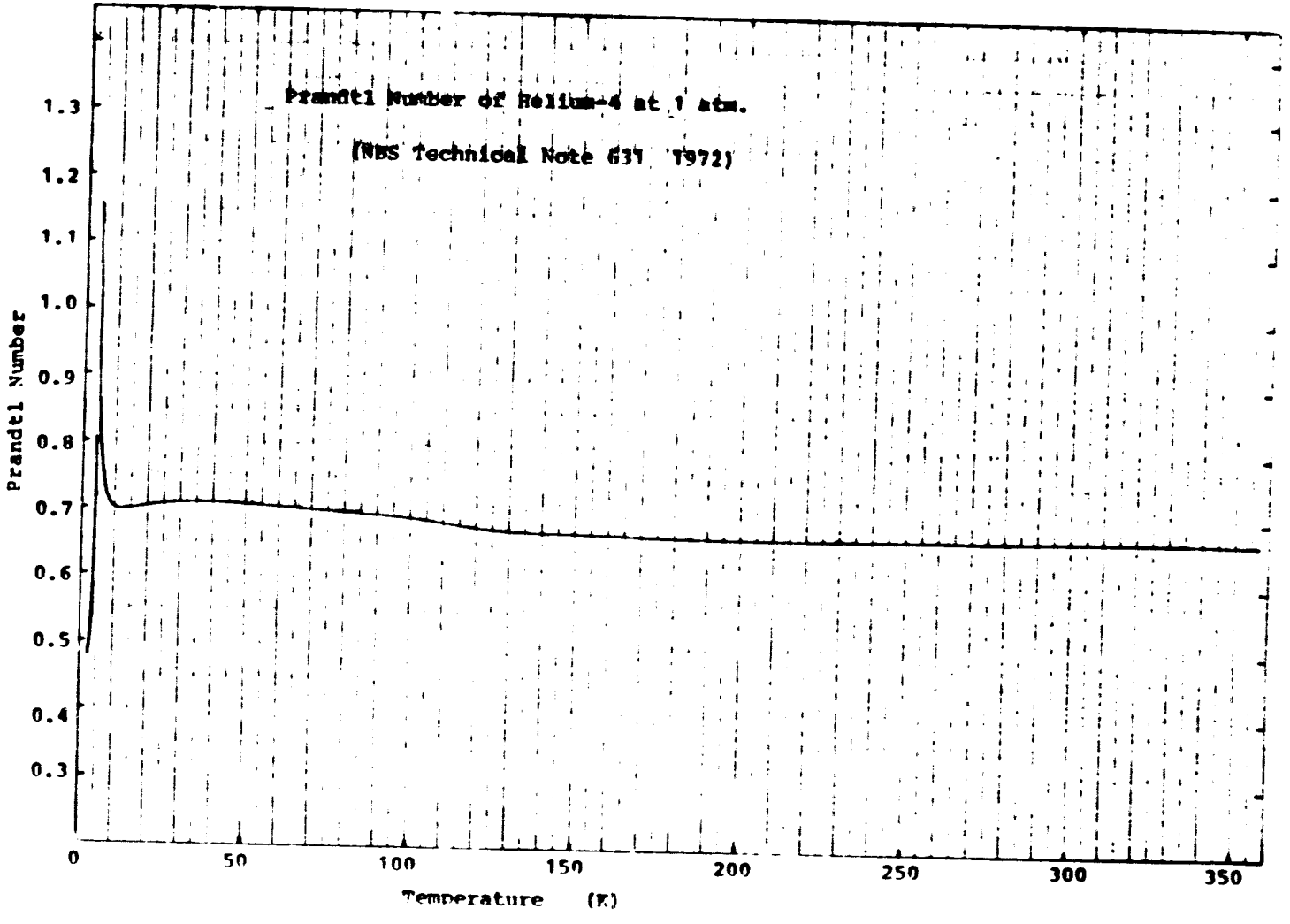

Figure A-5. Prandtl number of Helium-4 at 1 atm.

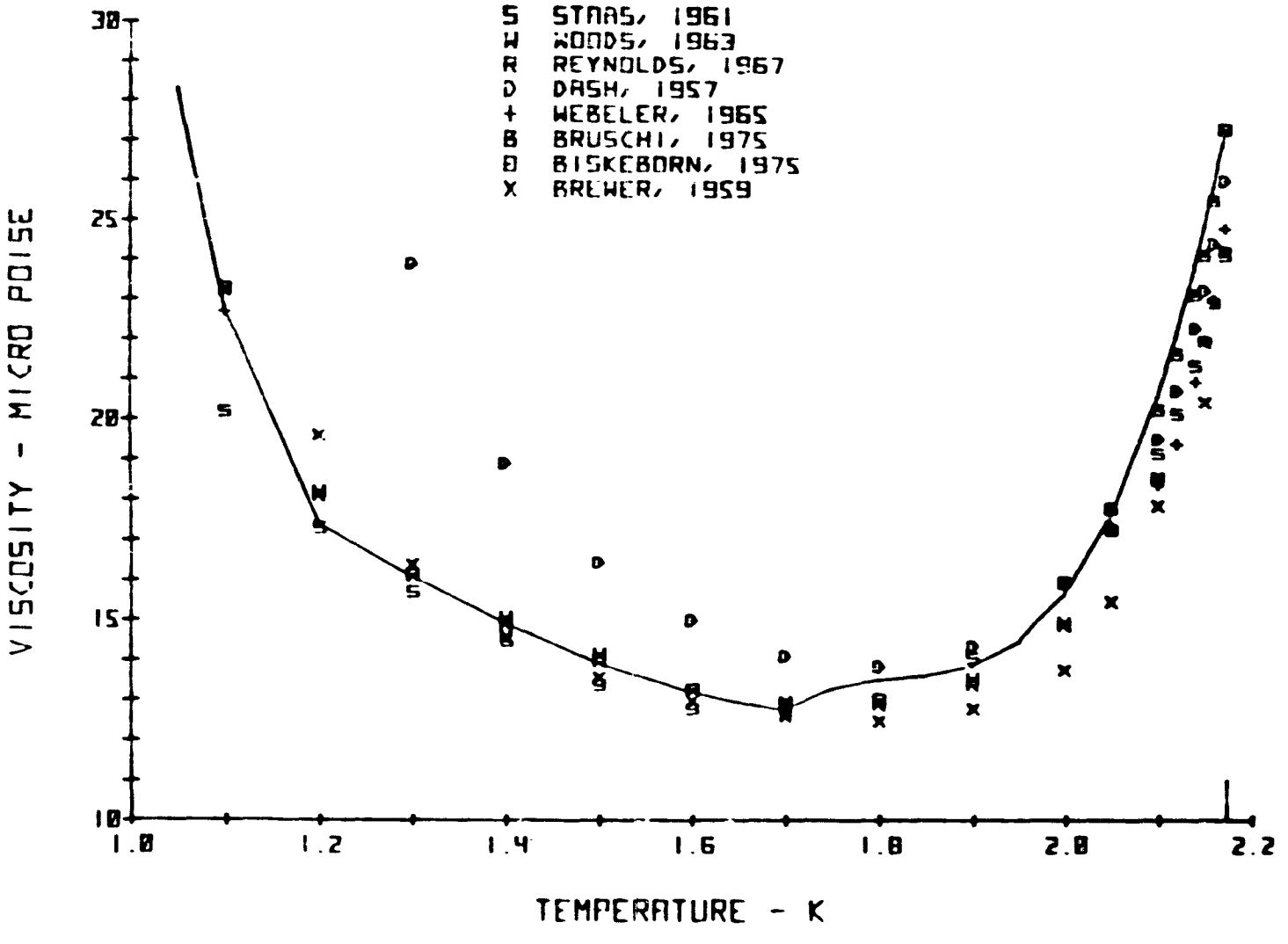

Fig. A.7. Normal fluid viscosity results $\eta_n(T)$ compiled by Soloski (Ph.D. thesis, UCLA,1977). List of authors in Table A-I.

TABLE A- I . Shear viscosity results $\eta_n(T)$
of the normal fluid of He II

S	Staas et al., Physica 27, 893, 1961
W	Woods et al., Can. J. Phys. 41, 596, 1963
R	Reynolds , Hussey, Goods, Phys. Fluids 10, 89, 1967
D	Dash - Taylor, Phys. Rev. 105, 7, 1957
+	Webeler - Hammer Phys. Letters, 15, 233, 1965
B	Bruschi et al. , J. Low Temp, Phys. 18, 487, 1975
◘	Biskeborn - Guernsey, Phys. Rev. Letters 34, 455, 1975.
x	Brewer et al., Proc. Roy. Soc. A 251, 247, 1959.

ABSTRACT

Continued studies are described in the area of vapor-liquid phase separator work with emphasis on permeabilities of porous sintered plugs (stainless steel, nominal pore size 2 μm). The temperature dependence of the permeability has been evaluated in classical fluid using He^4 gas at atmospheric pressure and in He II on the basis of a modified, thermo-osmotic permeability of the normal fluid.

KEYWORDS

Permeability , porous plug , He^4 gas , He II , thermo-osmosis, vapor-liquid phase separation.